that the AMPA receptor EPSC could be recorded in isolation (Fig. 2). Activation of NMDA receptors by the conditioning stimuli had no effect on the amplitude of the AMPA receptor test EPSC (100.1 ± 1.6%, n = 6). AMPA receptor EPSCs recorded in the presence of 2 mM extracellular Mg^{2+} to block NMDA receptor currents were not affected by 100 μM D-AP5 (n = 4).

In outside-out patches, the fast phase of development of glycine-insensitive desensitization is blocked by internal BAPTA, by ATP-γ-S, and by inhibitors of calcineurin (*7*). We used the same manipulations to block the synaptic form of desensitization. Although there was no difference in the amount of desensitization in recordings with 0.5 to 20 mM internal EGTA, 20 mM internal BAPTA blocked desensitization (Fig. 3, A and C). Addition of the specific inhibitors of calcineurin, cyclosporin A (200 to 500 nM), FK506 (200 to 500 nM), or calcineurin inhibitory peptide (270 μM) (*16*), blocked synaptic desensitization after 4 to 7 min of recording (Fig. 3, B and C). Synaptic desensitization was not prevented by calyculin A (200 nM), a phosphatase 1 and 2A inhibitor (*17*); by intracellular vanadate (1 mM), a tyrosine phosphatase inhibitor (*18*); or by phalloidin (1 μM), which stabilizes filamentous actin (*19*) and has been shown to prevent Ca^{2+}-dependent rundown of the NMDA receptor (*20*) (Fig. 3C). However, inclusion of 1 mM ATP-γ-S in the internal solution blocked desensitization within 4 to 6 min of the start of recordings (Fig. 3C).

These results indicate that the phosphorylation state of the NMDA receptor, or of an associated protein, alters NMDA receptor desensitization. Because synaptic desensitization is dependent on Ca^{2+} influx through NMDA receptor channels and subsequent activation of calcineurin, synaptic NMDA receptor complex may be dephosphorylated with each quantum of released transmitter. Inhibition of the effect of Ca^{2+} influx by chelation required the extremely fast binding properties of BAPTA (*21*); EGTA at concentrations that result in smaller amounts of free Ca^{2+} at equilibrium did not block synaptic desensitization. This observation suggests that the site of action of Ca^{2+} is very close to the cytoplasmic face of synaptic NMDA receptor channels. Calcineurin is reported to be associated with postsynaptic densities (*22*); this provides the spatial specificity for this mechanism.

Because recovery from desensitization requires several seconds, regulation of NMDA receptor function by this mechanism may be strong enough to significantly alter Ca^{2+}-dependent processes invoked by repetitive synaptic activity. The balance between homosynaptic LTD and LTP in the hippocampus depends in part on the magnitude of the increase of intracellular Ca^{2+} concentration as a result of influx through NMDA channels (*1–3*). Low-frequency stimulation (1 Hz) increases the intracellular Ca^{2+} concentration sufficiently to induce a calcineurin-dependent homosynaptic LTD (*2*), whereas high-frequency stimulation (100 Hz) raises Ca^{2+} to concentrations at which other Ca^{2+}-dependent reactions predominate and produce LTP (*3*). Thus, inhibition of induction of LTD by calcineurin blockers (*2*) may in part be a result of decreased NMDA receptor desensitization leading to greater intracellular Ca^{2+} concentrations during low-frequency stimulation.

REFERENCES AND NOTES

1. S. M. Dudek and M. F. Bear, *Proc. Natl. Acad. Sci. U.S.A.* **89**, 4363 (1992).
2. R. M. Mulkey *et al.*, *Nature* **369**, 486 (1994).
3. M. F. Bear and R. C. Malenka, *Curr. Opin. Neurobiol.* **4**, 389 (1994).
4. L.-Y. Wang *et al.*, *Nature* **369**, 230 (1994).
5. D. N. Lieberman and I. Mody, *ibid.*, p. 235.
6. Y. T. Wang and M. W. Salter, *ibid.*, p. 233.
7. G. Tong and C. E. Jahr, *J. Neurophysiol.* **72**, 754 (1994).
8. W. Sather *et al.*, *Neuron* **4**, 725 (1990); I. V. Chizhmakov *et al.*, *J. Physiol. (London)* **448**, 453 (1992).
9. R. A. J. Lester and C. E. Jahr, *J. Neurosci.* **12**, 635 (1992).
10. M. L. Mayer *et al.*, *ibid.* **7**, 3230 (1987); P. Ascher and L. Nowak, *J. Physiol. (London)* **399**, 247 (1988); C. E. Jahr and C. F. Stevens, *Nature* **325**, 522 (1987); C. Rosenmund *et al.*, *J. Neurophysiol.* **73**, 427 (1995).
11. J. M. Bekkers and C. F. Stevens, *Proc. Natl. Acad. Sci. U.S.A.* **88**, 7834 (1991). Whole-cell recordings of autaptic currents and miniature EPSCs were made (Axopatch-1D) with low-resistance patch pipettes (0.5 to 2.5 megohms) containing 150 mM potassium gluconate, 10 mM NaCl, 10 mM Hepes, 0.5 mM EGTA (except where noted), 4 mM magnesium adenosine triphosphate, and 0.2 mM guanosine triphosphate, adjusted to pH 7.3 with KOH. Control extracellular solution contained 160 mM NaCl, 3 mM KCl, 5 mM Hepes, 2 mM $CaCl_2$, 20 μM glycine, 5 μM 2,3-dihydroxy-6-nitro-7-sulfamoyl-benzo(F)quinoxaline (NBQX), and 50 to 100 μM picrotoxin, adjusted to pH 7.4 with NaOH. Autaptic EPSCs were evoked with voltage jumps to −20 or 0 mV from a holding potential of −60 to −90 mV (durations of 0.3 to 2 ms). Currents were sent through a low-pass filter at 0.5 to 10 kHz and were digitally sampled at 1 to 50 kHz. Series resistance compensation (80 to 100%) was used in all experiments. All experiments were performed at 22° to 24°C. Data are expressed as mean ± SEM.
12. The first two stimuli of the conditioning train were delivered 35 ms apart to allow for accurate measurement of the amplitude of the first EPSC. The second to fourth stimuli were delivered 20 ms apart.
13. Solution changes were made with gravity-fed flow tubes (*7, 9*).
14. N. A. Hessler *et al.*, *Nature* **366**, 569 (1993); C. Rosenmund *et al.*, *Science* **262**, 754 (1993).
15. C. E. Jahr and C. F. Stevens, *J. Neurosci.* **10**, 3178 (1990).
16. J. Kunz and N. N. Hall, *Trends Biochem. Sci.* **18**, 334 (1993); Y. Hashimoto, B. A. Perrino, T. R. Soderling, *J. Biol. Chem.* **265**, 1924 (1990). FK506 was added to the external solution, calcineurin inhibitory peptide was added to the internal solution, and cyclosporin A was added to both solutions.
17. H. Ishihara *et al.*, *Biochem. Biophys. Res. Commun.* **159**, 871 (1989). Calyculin A was added to the external solution.
18. G. Swarup *et al.*, *ibid.* **107**, 1104 (1982).
19. J. A. Cooper, *J. Cell Biol.* **105**, 1473 (1987).
20. C. Rosenmund and G. L. Westbrook, *Neuron* **10**, 805 (1993).
21. R. Pethig *et al.*, *Cell Calcium* **10**, 491 (1989).
22. S. Goto *et al.*, *Brain Res.* **397**, 161 (1986).
23. In two cells that exhibited the development of this current after washout of D-AP5, the frequencies of AMPA receptor spontaneous EPSCs (in the presence of D-AP5 and 2 mM Mg^{2+}) recorded after the four-pulse conditioning stimulus was delivered were two and four times, respectively, the unstimulated frequency. In an additional cell, the frequency increased to a point where spontaneous events summated and could not be counted. It is unlikely that free glutamate remained in the cleft after delivery of the conditioning stimulus because the D-AP5 was washed out in this interval; this result suggests that the synaptic clefts were well perfused.

24. Supported by NIH grant NS21419.

29 August 1994; accepted 21 December 1994

Storage of 7 ± 2 Short-Term Memories in Oscillatory Subcycles

John E. Lisman* and Marco A. P. Idiart

Psychophysical measurements indicate that human subjects can store approximately seven short-term memories. Physiological studies suggest that short-term memories are stored by patterns of neuronal activity. Here it is shown that activity patterns associated with multiple memories can be stored in a single neural network that exhibits nested oscillations similar to those recorded from the brain. Each memory is stored in a different high-frequency ("40 hertz") subcycle of a low-frequency oscillation. Memory patterns repeat on each low-frequency (5 to 12 hertz) oscillation, a repetition that relies on activity-dependent changes in membrane excitability rather than reverberatory circuits. This work suggests that brain oscillations are a timing mechanism for controlling the serial processing of short-term memories.

Some forms of short-term memory appear to be stored by neurons that continue to fire after they are excited by a brief input (*1*). Hebb and others (*2*) proposed that such firing is sustained by reverberation of electrical activity in neuronal loops. We now demonstrate the feasibility of an alternative mechanism that is based on known properties of hippocampal and cortical neurons: Firing is sustained by an increase in mem-

brane excitability (3, 4) that is refreshed on each cycle of a network oscillation. We also show that a simple oscillatory neuronal network that incorporates this mechanism can store multiple short-term memories, in accordance with psychophysical experiments showing that humans can store 7 ± 2 short-term memories (5). The model is based on the properties of known brain oscillations and suggests a specific role for these oscillations in memory function.

A mechanism by which firing can be maintained during short-term memory is suggested by recent biophysical measurements of the effects of acetylcholine and serotonin, neuromodulators that are released during periods of brain oscillation (6). In the absence of these neuromodulators, firing induces an afterhyperpolarization, which results in a transient decrease in excitability. However, in their presence, firing induces an afterdepolarization (ADP), which results in a transient increase in excitability (3). This ADP is too brief to account for the duration of short-term memory, but it is long enough to store information between cycles of oscillations in the theta-alpha range (5 to 12 Hz). Thus, if the ADP triggered in one cycle promoted firing in the next, the ADP would be refreshed during each cycle and firing could be maintained for many cycles. To examine this putative storage role of the ADP, we performed computer simulations. Each neuron (Fig. 1A) was assumed to receive a suprathreshold excitatory input that carries the information to be stored and an input that generates a subthreshold low-frequency oscillation. The simulations show (Fig. 1A) that after a neuron is excited by a single brief input, it fires on subsequent oscillatory cycles, thereby performing a storage function. A single memory could be stored by the spatial pattern of firing in a group of such neurons.

We next elaborated on this model to account for the ability of the brain to store approximately seven short-term memories (5) (Fig. 2A). An important clue regarding the underlying mechanisms is provided by experiments performed by Sternberg (7): A subject was exposed to a list of items and then to a test item. The subject pressed a button to indicate whether the test item was on the list and the reaction time was measured. For each additional item on the list, the reaction time increased by ~38 ms (Fig. 2B), an observation that is consistent with a serial scan process. This time increment corresponds to a cycle of a high-frequency brain oscillation in the beta-gamma range (8). If seven cycles of high-frequency oscillation were nested together by a low-frequency oscillation, the nesting oscillation would be in the range of alpha-theta oscillations (5 to 12 Hz). Thus, different memories may be stored in different high-frequency ("40 Hz") subcycles of a low-frequency oscillation. This possibility is strengthened by recent observations in cor-

J. E. Lisman, Department of Biology and Center for Complex Systems, Brandeis University, Waltham, MA 02254, USA.
M. A. P. Idiart, Department of Physics and Center for Complex Systems, Brandeis University, Waltham, MA 02254, USA.
*To whom correspondence should be addressed at: Center for Complex Systems, Brandeis University, Waltham, MA 02254, USA.

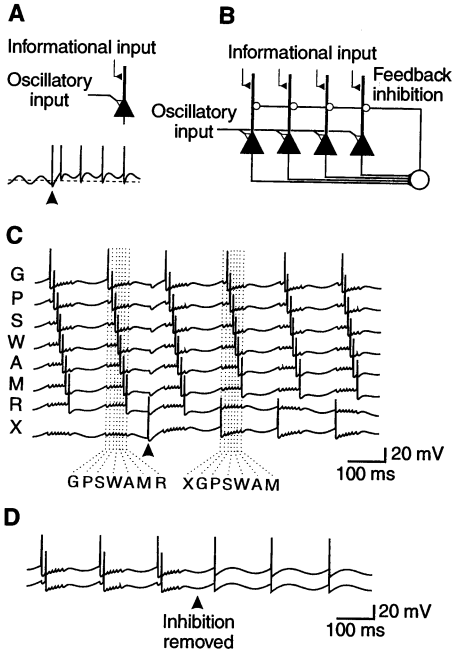

Fig. 1. (**A**) The ADP allows information storage in a single cell. The neuron receives a suprathreshold informational input and a second, subthreshold input that induces the membrane potential to oscillate at theta frequency (negative phase due to inhibition). Simulations (*23*) show membrane potential before and after informational input (arrowhead). (**B**) Network in which pyramidal cells make converging excitatory synapses onto an inhibitory interneuron that produces feedback inhibition of pyramidal cells. (**C**) The network can maintain the firing and correct phase of seven groups of cells that are active during different subcycles of the low-frequency oscillation. Each trace illustrates the synchronous firing of a group of cells whose spatial pattern encodes the memory of a letter. The dashed lines during the second and fourth theta cycles show the different subcycles. The limited memory capacity of the network is demonstrated by its failure to store eight memories. Input of the memory X is successful (arrowhead), but R is lost. (**D**) If feedback inhibition is removed (arrowhead), the "40-Hz" oscillation and phase information is rapidly lost. The two traces represent two of the seven memories stored in the network. A small phase difference (too small to be shown) persists for one cycle after removal of inhibition.

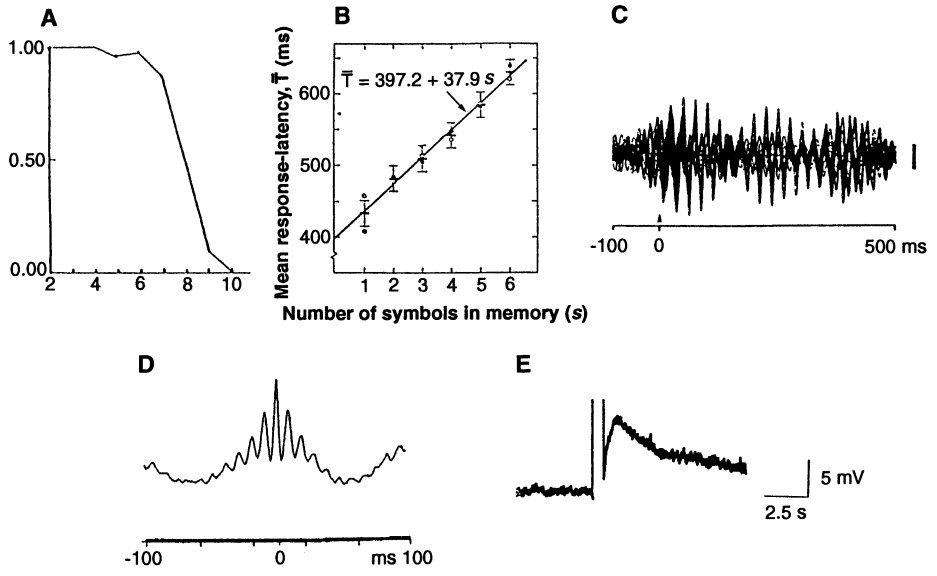

Fig. 2. Psychophysical and physiological data relevant to the model of short-term memory. (**A**) Human short-term memory capacity for list items. Probability of correct recall of entire list (*y* axis) as a function of list size (*x* axis). [Reproduced with permission from (*24*)] (**B**) Evidence for exhaustive serial scanning of the memory list. The subject responds if the test item is on the stored list. Response time is plotted as a function of the number of symbols in memory. [Reproduced with permission from (*7*)] (**C**) Nested oscillations demonstrated in a magnetoencephalographic recording of human cortical responses evoked by an acoustic stimulus. [Reproduced with permission from (*9*)] (**D**) Nested oscillations recorded from the hilar region of the rat hippocampus. The record is an average, triggered on high-frequency peaks of the waveform. [Reproduced with permission from Bragin *et al.* (*10*)] (**E**) ADP recorded with an intracellular microelectrode from a cortical pyramidal cell. The large initial deflection is due to a current pulse that evokes action potentials. After the end of current injection, the ADP rises slowly and then falls (previously unpublished record provided by R. Andrade).

tex (Fig. 2C) and hippocampus (Fig. 2D) showing that approximately seven high-frequency subcycles are nested in a low-frequency oscillation (*9*, *10*).

Could the ADP provide a mechanism for storing different memories in different subcycles? An important feature of the ADP is its slow rise (Fig. 2E). The most excitable cells are therefore not those that just fired, but those that fired earliest. More specifically, the most excitable cells in the first subcycle of a low-frequency oscillation would be those that fired on the first subcycle of the previous low-frequency cycle. Similarly, the most excitable cells in the second subcycle would be those that fired on the second subcycle of the previous cycle. The slow increase in the ADP thus provides ramps of excitation that could serve as a basis for ordering multiple memories (*11*). Figure 1B shows a network of cells, each of which can generate an ADP. The neurons receive continuous oscillatory input and pooled feedback inhibition (*10*), the function of which is to partition a cycle into subcycles. The first part of the simulation (Fig. 1C, left of arrowhead) shows that a network with these properties can faithfully store seven nonoverlapping (*12*) memories. The memories were previously loaded into the network by brief activation of informational inputs. Each memory is represented by a group of cells that fire simultaneously during a particular subcycle. When a different group of cells is briefly presented with the eighth pattern, X, at its informational inputs (Fig. 1C, arrowhead), this group then fires on the first subcycle of each subsequent cycle. Previous memories are shifted back one subcycle, and the memory pattern stored in the last subcycle, R, is lost [for alternative assumptions and ideas concerning readout, see (*13*, *14*)]. The number of memories that can be stored without loss depends on variables that we have adjusted in order to limit the number to seven, in accord with average human performance (*5*). This simulation demonstrates that the network shown in Fig. 1B can store multiple memories and keep them separate by phase (oscillatory subcycles). The number of short-term memories that can be stored is limited by the number of subcycles that fit within a low-frequency cycle. In the model, the presence of subcycles is dependent on the feedback inhibition (Fig. 1D).

Systematic changes in the phase of cell firing occur as new information is introduced into the network (Fig. 1C). The observation of systematic phase changes in hippocampal place cells (*15*) thus suggests that the storage mechanism we have modeled may be applicable to the hippocampus. A second important feature of the model is the property of time compression: Sequential memories inserted over many seconds are recreated in the network at intervals of ~25 ms (Fig. 1C). Such compression might enable the *N*-methyl-D-aspartate subtype of glutamate receptor channel, which exhibits an associational mechanism with a 100-ms time scale, to form associations between events that occurred at much greater intervals.

Our model is consistent with the previous proposal (*16*, *17*) that the phase of cell firing in oscillatory networks can be used to distinguish different activity patterns. However, our model predicts that cells are not likely to fire on sequential 40-Hz subcycles because different subcycles represent different information. The available data appear consistent with this view (*18*) and recent experiments show directly that sequential 40-Hz waves relate to different rather than identical perceptual information (*19*). Another prediction is that memory patterns repeat on each low-frequency brain oscillation. Consistent with this view is the observation that brief sensory stimulation or cortical electrical stimulation produces electroencephalogram afterdischarges that repeat at the low-frequency, alpha rhythm (*20*). The model could be further tested by artificially exciting single cells. Because the proposed memory mechanism is based on an intrinsic neuronal property, the ADP, the model predicts that a cell should continue to fire on subsequent oscillatory cycles. The analysis of electrical events during short-term memory tasks (*21*) should provide a further basis for testing the ideas proposed here.

Note added in proof: We have recently become aware of a report (*22*) showing oscillatory activity ~4 Hz during a short-term memory task.

REFERENCES AND NOTES

1. J. M. Fuster and J. P. Jervey, *J. Neurosci.* **2**, 361 (1982); S. Funahashi, C. J. Bruce, P. S. Goldman-Rakic, *J. Neurophysiol.* **61**, 331 (1989).
2. D. O. Hebb, *The Organization of Behavior* (Wiley, New York, 1949); D. J. Amit, *Modeling Brain Function* (Cambridge Univ. Press, Cambridge, 1989); D. J. Amit, N. Brunel, M. V. Tsodyks, *J. Neurosci.* **14**, 6435 (1994); D. Zipser, B. Kehoe, G. Littlewort, J. Fuster, *ibid.* **13**, 3406 (1993).
3. Cholinergic induction of an ADP is described by R. Andrade [*Brain Res.* **548**, 81 (1991)], M. Caeser, D. A. Brown, B. H. Gahwiler, and T. Knopfel [*Eur. J. Neurosci.* **5**, 560 (1993)], and J. F. Storm [*J. Physiol. (London)* **409**, 171 (1989)]. The similar effects of serotonin are described by R. Araneda [*Neuroscience* **40**, 399 (1991)].
4. D. Horn and M. Usher [*Neural Comput.* **3**, 31 (1991); in *Advances in Neural Information Processing Systems*, J. E. Moody, S. J. Hanson, P. Lippmann, Eds. (Morgan & Kaufmann, San Mateo, CA, 1994), vol. 4, pp. 125–132] explore related ideas concerning the retrieval of multiple memories by oscillatory networks.
5. G. A. Miller, *Psychol. Rev.* **63**, 81 (1956).
6. Interaction of the ADP with brain oscillations is likely, given (*3*) and the evidence for the participation of acetylcholine and serotonin in brain oscillations [M. Steriade, R. Curro Dossi, D. Pare, G. Oakson, *Proc. Natl. Acad. Sci. U.S.A.* **88**, 4396 (1991); B. Bland, *Prog. Neurobiol.* **26**, 1 (1986)].
7. S. Sternberg, *Science* **153**, 652 (1966).
8. Scan time/memory (s = 38 ms/memory) (*6*) may be the sum of true scan time/memory and a time, T/memory, imposed by other costs of increasing complexity. T = 13 ms/memory can be estimated when the number of memories exceeds capacity from the data of D. Burrows and R. Okada [*Science* **188**, 1031 (1975)]. In this instance, true retrieval time/memory would equal 25 ms (38 ms − 13 ms) and implicate a 40-Hz oscillation.
9. R. Llinas and U. Ribary, *Proc. Natl. Acad. Sci. U.S.A.* **90**, 2078 (1993).
10. A. Bragin *et al.*, *J. Neurosci.* **15**, 47 (1995). A related study showing both theta and 40-Hz oscillations was performed by I. Soltesz and M. Deschenes [*J. Neurophysiol.* **70**, 97 (1993)].
11. If additional spikes are superposed on an existing ADP, a hyperpolarizing event is evoked. This after-hyperpolarization decays within 500 ms, thereby generating a positive ramp to a final depolarized level (R. Andrade, personal communication). It is therefore reasonable to model the upward ramp of the ADP as being reinitiated with each spike.
12. With nonoverlapping memories, a given cell only participates in a single pattern. If memories overlap, cells should fire on multiple subcycles. However, the ADP could only cause firing on one subcycle. The "missing" signal could conceivably be filled in if recurrent modifiable excitatory collaterals are present (*17*). Understanding such collaterals is also of importance to the transition to long-term memory and to the formation of associations between different memory patterns. The ADP and rapidly modifiable synapse may both be involved in short-term memory.
13. As modeled, loss of previous memories occurs as a direct result of entry of new information. There is some support for such an effect in human memory [R. C. Atkinson and R. M. Shiffrin, in *The Psychology of Learning and Motivation: Advances in Research and Theory*, K. W. Spence, and J. T. Spence, Eds. (Academic Press, San Diego, CA, 1968), vol. 2, pp. 89–105]. Alternatively, some psychological measurements are more consistent with a passive decay process [A. Wingfield and D. L. Byrnes, *Science* **176**, 690 (1972)]. If one assumes a sharp decay process after ~1.5 s and the loading of new memories at the end of the memory stack, the phase of memory becomes earlier as new memories are entered, rather than later as in Fig. 1C.
14. Further assumptions are required to predict reaction time during memory readout in the Sternberg task. One model is that presentation of the test item resets the low-frequency oscillation and initiates the sequential readout of memory-containing subcycles; the greater the number of subcycles that contain memories, the longer the reaction time.
15. J. O'Keefe and M. L. Recce, *Hippocampus* **3**, 317 (1993); W. E. Skaggs, M. A. Wilson, B. L. McNaughton, *Soc. Neurosci. Abstr.* **19**, 795 (1993). Phase of firing advances with time [for comparison see (*13*)].
16. W. Singer, *Annu. Rev. Physiol.* **55**, 349 (1993).
17. C. von der Malsburg, *Biol. Cybernet.* **54**, 29 (1986).
18. There is some indication that cells can fire on multiple sequential cycles of 40-Hz oscillations [A. K. Kreiter and W. Singer, *Eur. J. Neurosci.* **4**, 369 (1992)], but generally this has not been observed [C. Koch and F. Crick, in *Some Further Ideas Regarding the Neuronal Basis of Awareness in Large Scale Neuronal Theories of the Brain*, C. Koch and J. L. Davis, Eds. (MIT Press, Cambridge, MA, 1994), pp. 93–109.
19. M. Joliot, U. Ribary, R. Llinas, *Proc. Natl. Acad. Sci. U.S.A.* **91**, 11748 (1994).
20. H.-T. Chang, *J. Neurophysiol.* **13**, 235 (1950).
21. A crucial question that remains unclear is whether spike trains recorded during memory tasks (*1*) are dependent on an oscillatory storage process. Simultaneous recordings of spike trains and field potentials, as in (*15*), may be required to settle this issue. Magnetoencephalographic and electroencephalo-

gram measurements during short-term memory tasks are described by L. Kaufman, S. Curtis, J. Z. Wang, and S. J. Williamson [*Electroencephalogr. Clin. Neurophysiol.* **82**, 266 (1992)] and M. Fahle, J. Albrecht, H. Buelthoff, and D. Braun [*Soc. Neurosci. Abstr.* **20**, 319 (1994)].

22. K. Nakamura, A. Mikami, K. Kubota, *Neuroreports* **3**, 117 (1992).
23. Pyramidal cells are modeled as identical integrate-and-fire neurons. The membrane potential for each pyramidal cell is given by

$$\tau_v dV_i(t)/dt = -V_i(t) + V^{rest} + V^{osc}(t) + V_i^{ADP}(t) + V^{inh}(t)$$

and it is reset to $V^{rest} = -60$ mV when it exceeds $V^{thresh} = -50$ mV, the threshold for spike generation. Because it does not change the qualitative features of the model, we assume that τ_v is small compared to any other time constant, so that

$$V_i(t) \approx V_{rest} + V^{osc}(t) + V_i^{ADP}(t) + V^{inh}(t)$$

The inhibitory interneuron is not explicitly modeled; it is activated by each spike in a pyramidal cell and it inhibits all pyramidal cells. This inhibition is assumed to be a linear superposition of inhibitory postsynaptic potentials, such that $V^{inh}(t) = \Sigma\, \alpha(t - t_n)$, where t_n is the time of the nth spike in the network and α is the alpha function, $\alpha(t) = A^*(t/\tau)^*\exp(1 - t/\tau)$, with $A^{inh} = -4$ mV and $\tau^{inh} = 5$ ms. V_i^{ADP} increases from zero after each action potential in cell i (*11*) with an alpha function of amplitude $A^{ADP} = 10$ mV and a time constant of $\tau^{ADP} = 200$ ms. The oscillatory input is $V^{osc}(t) = B^*\sin(2\pi ft)$, with $f = 6$ Hz and $B = 5$ mV. A memory is inserted through informational inputs at a single negative peak of the cycle. The brief input is sufficient to activate the cells and evoke an ADP.

24. H. S. Oberly, *Am. J. Psychol.* **40**, 295 (1928).
25. Supported by the W. M. Keck Foundation and NIH grant NS27337. We thank L. Abbott, S. Sternberg, G. Buzsaki, and M. Kahana for extensive discussions. We extend special thanks to R. Llinas for pointing out Miller's work on memory limits.

13 September 1994; accepted 5 January 1995

TECHNICAL COMMENTS

Interhelical Angles in the Solution Structure of the Oligomerization Domain of p53: Correction

We recently presented the solution structure of the oligomerization domain (residues 319–360) of the tumor suppressor p53 using an multidimensional heteronuclear-edited and -filtered nuclear magnetic resonance (NMR) spectroscopy (*1*). The structure comprised a dimer of dimers, each dimer being formed by two antiparallel helices and an antiparallel β sheet. The two dimers were arranged approximately orthogonal to each other such that the tetramer formed a four-helical bundle with the antiparallel β sheets lying on opposing faces of the molecule. After the determination of the NMR structure, the crystal structure of the oligomerization domain was solved by Nikola Pavletich and his colleagues and kindly provided to us for comparison (*2*). While the overall topology of the tetramer was the same in the NMR and x-ray structures, a difference in the orientation of the two dimers (that is between the AC dimer and the BD dimer) was observed. Specifically, the angle between the long axes of helices A and B was 114° in the solution structure versus 80° in the crystal structure. Thus, while the structure of the dimer was similar, the root-mean-square (rms) difference between our proposed NMR structure and the x-ray structure for the complete tetramer was large (3 Å). This difference involves a rigid body rotation of one dimer relative to the other about the symmetry axis of the tetramer and is readily appreciated from the ribbon diagrams of the original NMR structure and the x-ray structure (Fig. 1, A and B, respectively). It is important to determine whether a genuine difference between solution and crystal structures exists, or whether a misinterpretation of the NMR data could be the cause of this discrepancy.

To this end, we reexamined our nuclear Overhauser enhancement (NOE) data obtained from both the four-dimensional (4D) $^{13}C/^{13}C$-separated and three-dimensional (3D) ^{13}C-separated/^{12}C-filtered NOE spectra. We found that, although the partitioning of the intersubunit NOEs was correct, there were three errors in NOE assignments involving contacts between the A and B subunits (and by symmetry between the C and D subunits). Specifically, the weak NOEs between Lys^{351} CεH(A) and Met^{340}-CγH(B), Lys^{351}CδH(A) and Met^{340}-CαH(B), and Lys^{351}CγH(A) and Met^{340}-CαH(B), which were only identified in the 4D $^{13}C/^{13}C$-separated NOE spectrum, were a

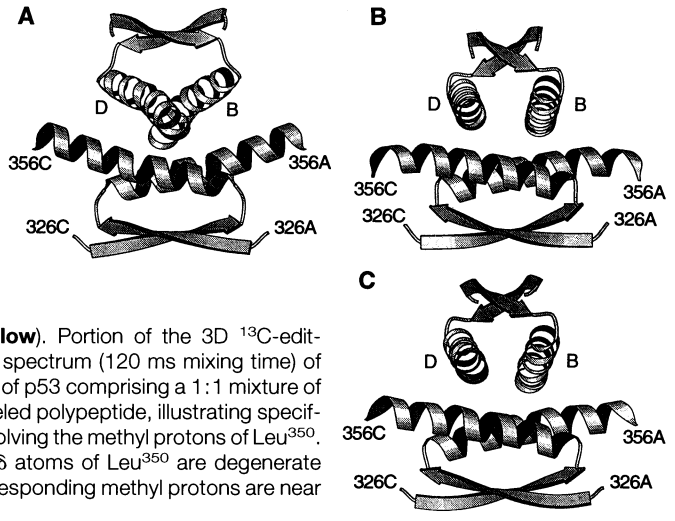

Fig. 1 (right). Ribbon diagrams of (**A**) the original average NMR structure, (**B**) the x-ray structure, and (**C**) the new average NMR structure (*3*). The angle between helices A and B, which describes the orientation of the two dimers, is 114° in (A), 80° in (B), and 78° in (C). The figure was generated with the program MOLSCRIPT (*7*).

Fig. 2 (below). Portion of the 3D ^{13}C-edited(F_2)/^{12}C-filtered(F_3) NOE spectrum (120 ms mixing time) of the oligomerization domain of p53 comprising a 1:1 mixture of unlabeled and $^{13}C/^{15}N$-labeled polypeptide, illustrating specifically intersubunit NOEs involving the methyl protons of Leu^{350}. The ^{13}C shift of the two Cδ atoms of Leu^{350} are degenerate and the ^1H shifts of the corresponding methyl protons are near degenerate.